

# Nighttime dissolution in a temperate coastal ocean ecosystem increases under acidification: Supplementary material

Lester Kwiatkowski<sup>1\*</sup>, Brian Gaylord<sup>2</sup>, Tessa Hill<sup>2</sup>, Jessica Hosfelt<sup>2</sup>, Kristy J. Kroeker<sup>2,3</sup>, Yana Nebuchina<sup>1</sup>, Aaron Ninokawa<sup>2</sup>, Ann Russell<sup>2</sup>, Emily B. Rivest<sup>2</sup>, Marine Sesboüé<sup>1</sup>, Ken Caldeira<sup>1</sup>

<sup>1</sup> Department of Global Ecology, Carnegie Institution for Science, 260 Panama Street, Stanford, California, 94305, USA;

<sup>2</sup> Bodega Marine Laboratory, University of California, Bodega Bay, California, 94923, USA;

<sup>3</sup> Center for Ocean Health, 100 Shaffer Road, University of California, Santa Cruz, California, 95064, USA.

## Abbreviations

$A_T$	Total alkalinity
$C_T$	Dissolved Inorganic Carbon
$G_{net}$	Net community calcification
$P_{net}$	Net community production
$\Omega_{arag}$	Aragonite saturation state
PAR	Photosynthetically active radiation
$PAR_{mm}$	Michaelis-Menten function of PAR
$T_f$	Gaussian function of temperature
$F_{CO_2}$	Air-sea flux of $CO_2$
$\rho$	Sea water density
$d$	Mean tide pool depth

## Collinearity between explanatory variables

Table S1. Variance Inflation factors (VIFs) for the potential explanatory variables in each tide pool during the day.

	$PAR_{mm}$	$P_{net}$	$T_f$	$\Omega_{arag}$
<b>Pool 1</b>	5.48	2.00	4.32	1.28
<b>Pool 2</b>	2.49	1.22	1.64	2.15
<b>Pool 3</b>	6.45	2.25	5.04	4.00
<b>Pool 4</b>	3.07	2.69	2.11	2.26

Table S2. Variance Inflation factors (VIFs) for the potential explanatory variables in each tide pool during the night.

	$P_{net}$	$T_f$	$\Omega_{arag}$
<b>Pool 1</b>	1.55	1.52	2.15
<b>Pool 2</b>	2.12	1.21	2.34
<b>Pool 3</b>	1.97	1.72	2.53
<b>Pool 4</b>	1.58	1.61	2.03

Table S3. Pearson correlation coefficients between explanatory variables in each tide pool during the day.

		<b>PAR<sub>mm</sub></b>	<b>P<sub>net</sub></b>	<b>T<sub>f</sub></b>	<b>Ω<sub>arag</sub></b>
<b>Pool 1</b>	<b>PAR<sub>mm</sub></b>	1			
	<b>P<sub>net</sub></b>	0.70	1		
	<b>T<sub>f</sub></b>	0.87	0.58	1	
	<b>Ω<sub>arag</sub></b>	0.43	0.29	0.46	1
<b>Pool 2</b>	<b>PAR<sub>mm</sub></b>	1			
	<b>P<sub>net</sub></b>	-0.09	1		
	<b>T<sub>f</sub></b>	0.58	0.18	1	
	<b>Ω<sub>arag</sub></b>	0.70	-0.29	0.37	1
<b>Pool 3</b>	<b>PAR<sub>mm</sub></b>	1			
	<b>P<sub>net</sub></b>	0.40	1		
	<b>T<sub>f</sub></b>	0.88	0.33	1	
	<b>Ω<sub>arag</sub></b>	0.71	-0.15	0.71	1
<b>Pool 4</b>	<b>PAR<sub>mm</sub></b>	1			
	<b>P<sub>net</sub></b>	0.53	1		
	<b>T<sub>f</sub></b>	0.37	0.71	1	
	<b>Ω<sub>arag</sub></b>	0.61	-0.03	-0.12	1

Table S4. Pearson correlation coefficients between explanatory variables in each tide pool during the night.

		<b>P<sub>net</sub></b>	<b>T<sub>f</sub></b>	<b>Ω<sub>arag</sub></b>
<b>Pool 1</b>	<b>P<sub>net</sub></b>	1		
	<b>T<sub>f</sub></b>	-0.09	1	
	<b>Ω<sub>arag</sub></b>	-0.55	0.53	1
<b>Pool 2</b>	<b>P<sub>net</sub></b>	1		
	<b>T<sub>f</sub></b>	-0.02	1	
	<b>Ω<sub>arag</sub></b>	-0.70	0.31	1
<b>Pool 3</b>	<b>P<sub>net</sub></b>	1		
	<b>T<sub>f</sub></b>	0.09	1	
	<b>Ω<sub>arag</sub></b>	-0.57	0.48	1
<b>Pool 4</b>	<b>P<sub>net</sub></b>	1		
	<b>T<sub>f</sub></b>	0.12	1	
	<b>Ω<sub>arag</sub></b>	-0.46	0.48	1

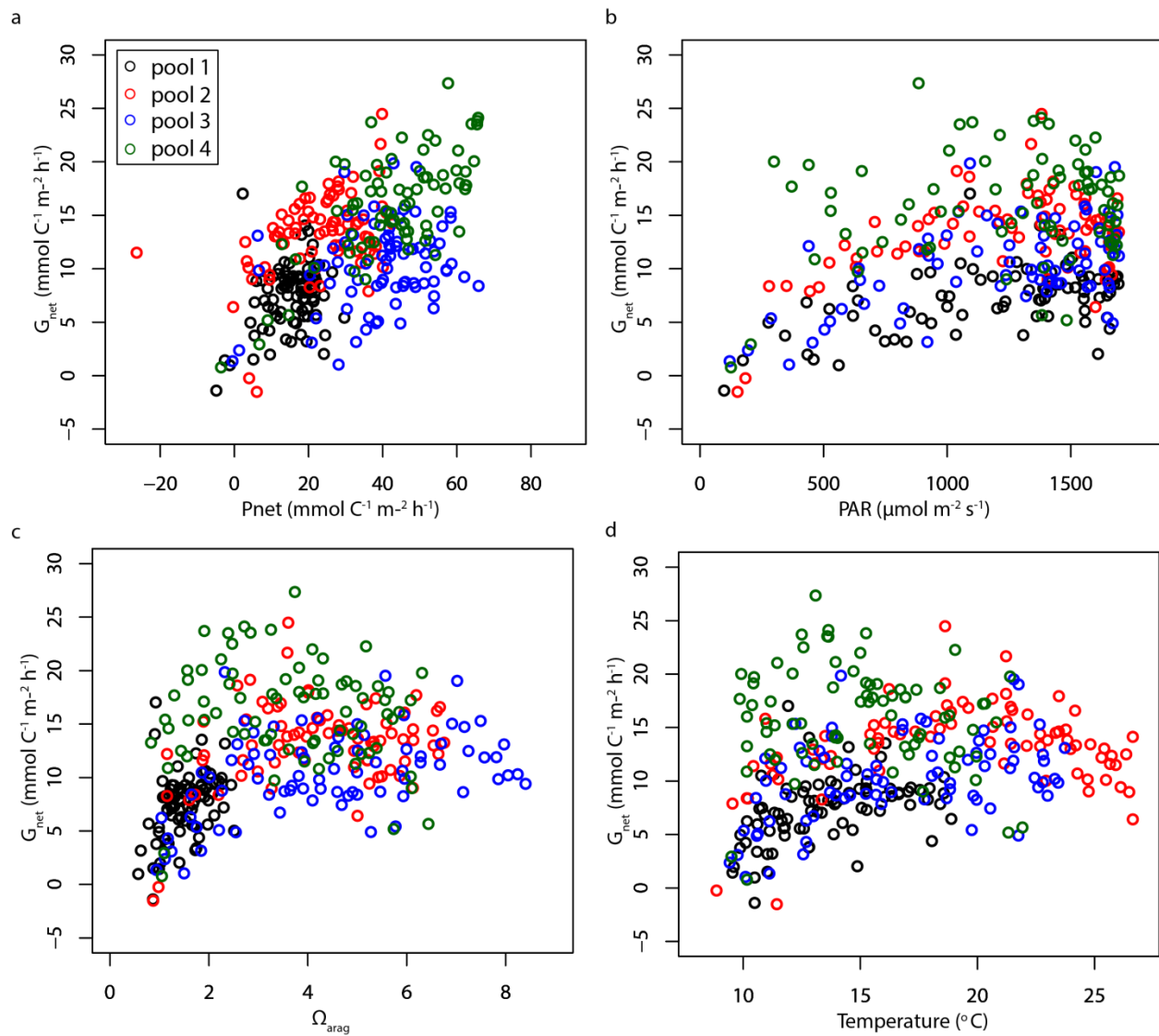


Figure S1.  $G_{\text{net}}$  ( $\text{mmol C}^{-1} \text{m}^{-2} \text{h}^{-1}$ ) against a,  $P_{\text{net}}$  ( $\text{mmol C}^{-1} \text{m}^{-2} \text{h}^{-1}$ ), b, Photosynthetically Active Radiation ( $\mu\text{mol m}^{-2} \text{s}^{-1}$ ), c, Aragonite saturation state ( $\Omega_{\text{arag}}$ ) and d, Temperature ( $^{\circ}\text{C}$ ) in each of the tide pools during the day.

## Nutrients

The concentration of  $\text{NO}_2^- + \text{NO}_3^-$  is found to generally decrease between the first and last bottle samples on a given sample day (daylight hours; Fig. S2). Although this may be representative of net community nutrient  $\text{NO}_2^- + \text{NO}_3^-$  uptake, the magnitude of changes are orders of magnitude lower than changes in  $\Delta A_7$  and therefore any corresponding net community release of anions<sup>1,2,3</sup> would have negligible influence on  $G_{\text{net}}$ . The rate of change of  $\text{NH}_3 + \text{NH}_4^+$  concentration between first and last daily bottle samples is shown to be highly variable (Fig. S2). However measured  $\Delta(\text{NH}_3 + \text{NH}_4^+)$  explains none of the variance in  $\Delta A_7$  (Fig. S3). As such, sporadic high concentrations are interpreted as a consequence of local animal excretion and not a result of net community uptake. The release of  $\text{H}^+$  associated with the latter would have had a strong influence on measured  $A_7$ <sup>1,2,3</sup>. We therefore conclude that  $\Delta A_7$  is primarily driven by community calcification. Nutrient concentrations were not measured for nighttime samples.

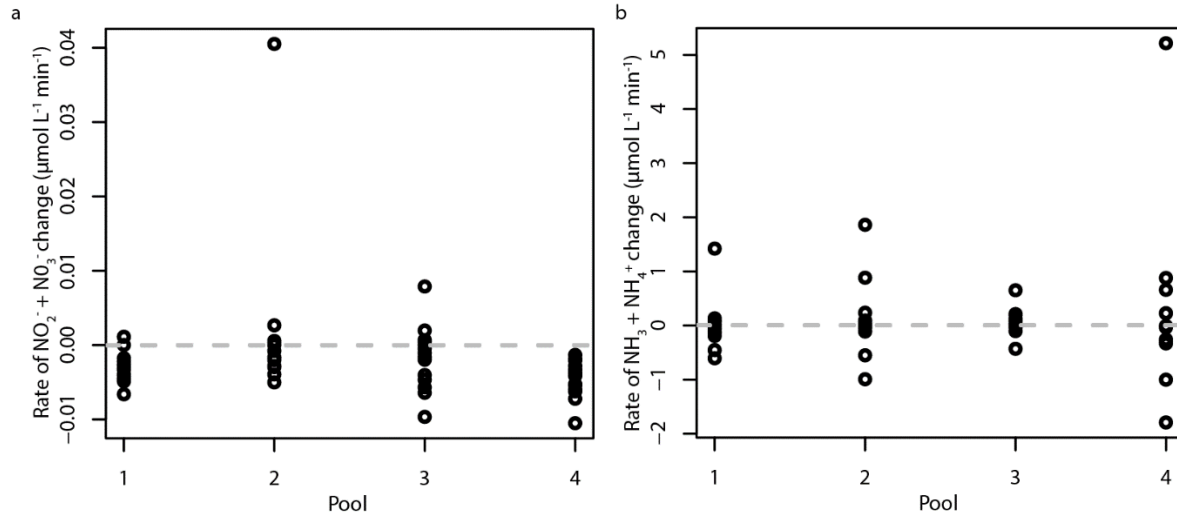


Figure S2. Rate of a,  $\text{NO}_2^- + \text{NO}_3^-$  and b,  $\text{NH}_3 + \text{NH}_4^+$  concentration change between first and last daily sampling times in each tide pool ( $\mu\text{mol L}^{-1} \text{min}^{-1}$ ). All samples were taken during the daytime.

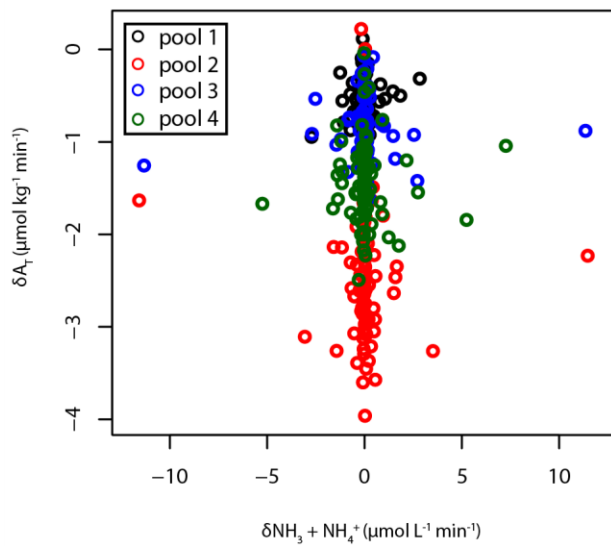


Figure S3.  $\delta\text{NH}_3 + \text{NH}_4^+$  ( $\mu\text{mol L}^{-1} \text{min}^{-1}$ ) against  $\delta A_T$  ( $\mu\text{mol kg}^{-1} \text{min}^{-1}$ ) in each tide pool. There is no significant relationship between  $\delta\text{NH}_3 + \text{NH}_4^+$  and  $\delta A_T$  in any of the tide pools.

## PAR and temperature functions

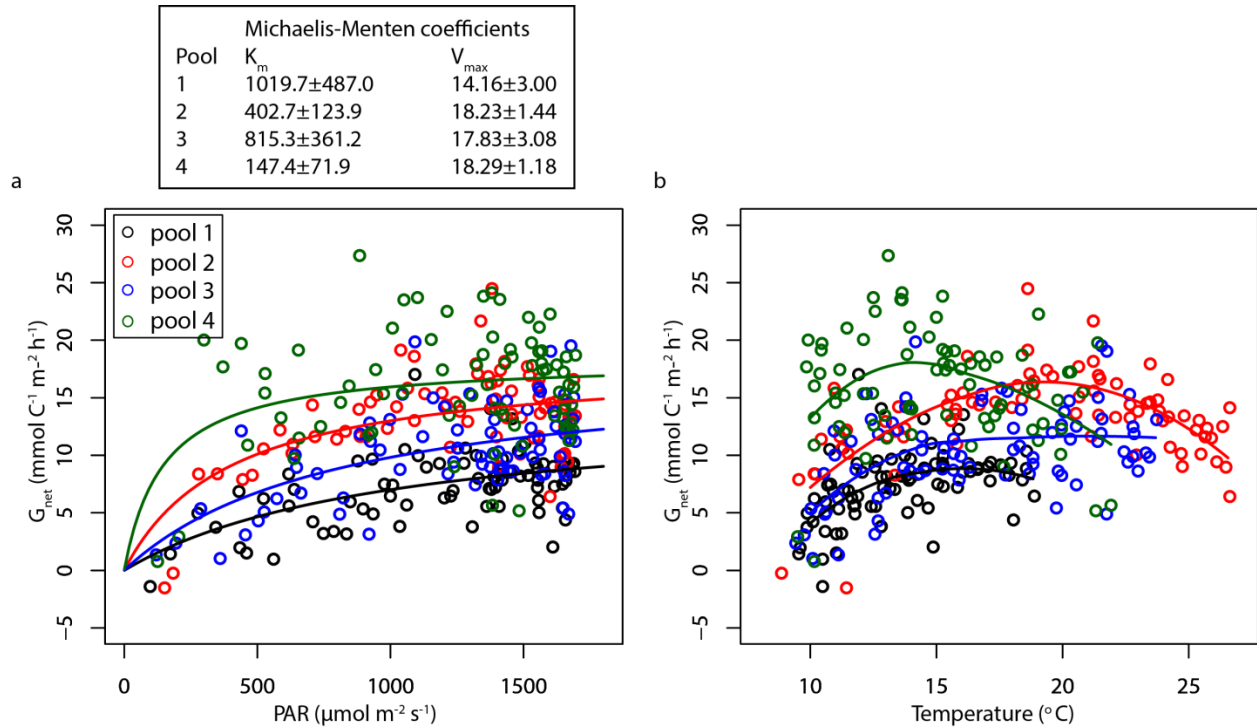


Figure S4.  $G_{net}$  ( $\text{mmol C}^{-1} \text{m}^{-2} \text{h}^{-1}$ ) against a, PAR ( $\mu\text{mol m}^{-2} \text{s}^{-1}$ ) and b, temperature ( $^{\circ}\text{C}$ ) in each of the tide pools. Michaelis-Menten and Gaussian functions are derived for  $G_{net}$ -PAR and  $G_{net}$ -temperature relationships respectively. Michaelis-Menten ( $V = V_{max}[S]/(K_m + [S])$ ) coefficients with associated standard errors are given however as the Gaussian temperature functions are produced using locally weighted regression methods (LOESS)<sup>4</sup> they cannot be represented by a simple mathematical equation.

## Alkalinity-dissolved inorganic carbon relationships

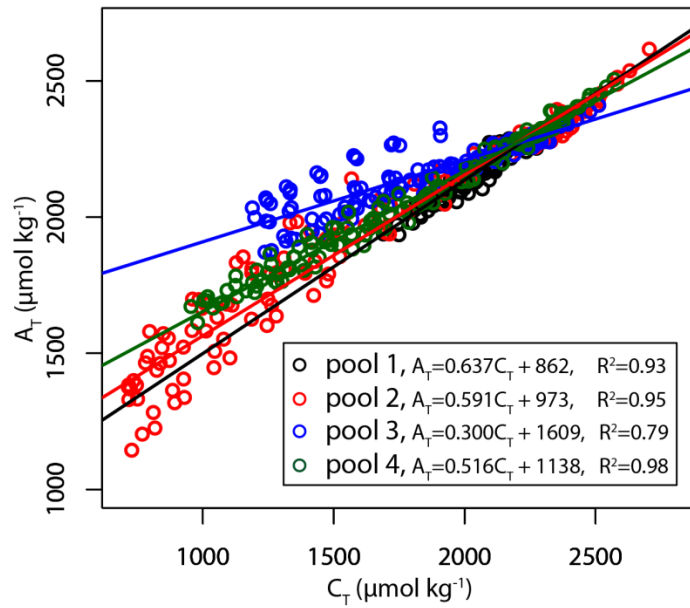


Figure S5. Total least squares regressions between alkalinity ( $A_T$ ) and dissolved inorganic carbon ( $C_T$ ) in each of the tide pools.



## Nighttime community calcification against $P_{\text{net}}$ and temperature

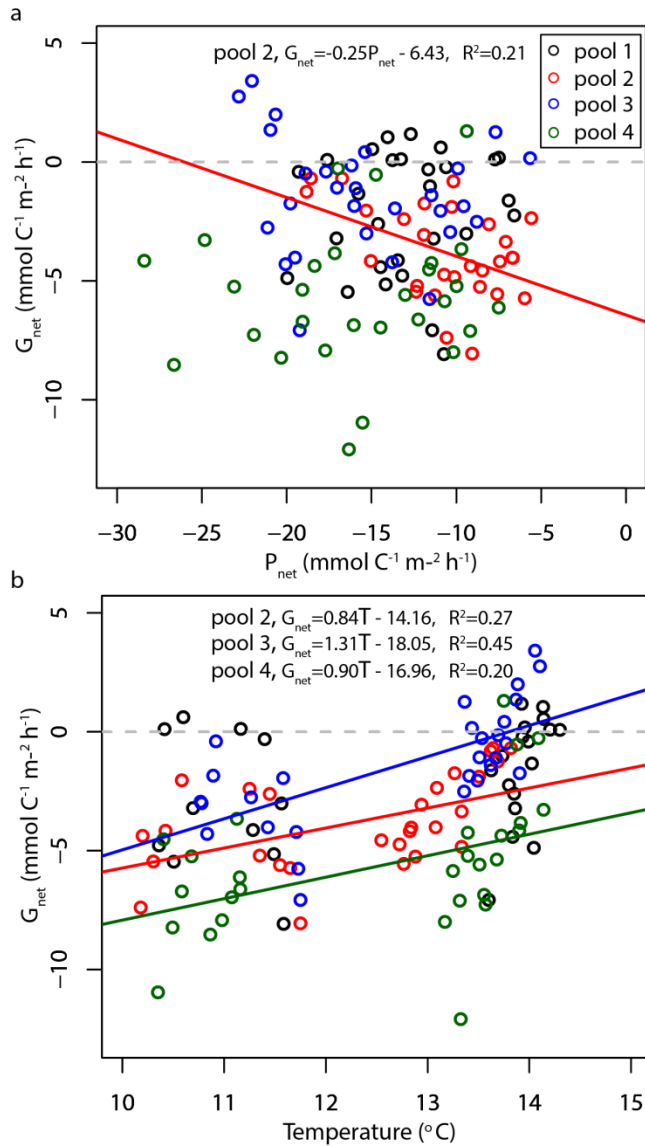


Figure S6. Nighttime  $G_{\text{net}}$  ( $\text{mmol C}^{-1} \text{m}^{-2} \text{h}^{-1}$ ) against a,  $P_{\text{net}}$  ( $\text{mmol C}^{-1} \text{m}^{-2} \text{h}^{-1}$ ), and b, Temperature ( $^{\circ}\text{C}$ ) in each of the tide pools. Regression lines of variables significant at the  $p < 0.05$  level are shown. Dashed grey lines show the separation between net community calcification and net community dissolution.

## References

1. Brewer, P. G. & Goldman, J. C. Alkalinity changes generated by phytoplankton growth1. *Limnol. Oceanogr.* **21**, 108–117 (1976).
2. Goldman, J. C. & Brewer, P. G. Effect of nitrogen source and growth rate on phytoplankton-mediated changes in alkalinity1. *Limnol. Oceanogr.* **25**, 352–357 (1980).
3. Wolf-Gladrow, D. A., Zeebe, R. E., Klaas, C., Körtzinger, A. & Dickson, A. G. Total alkalinity: The explicit conservative expression and its application to biogeochemical processes. *Mar. Chem.* **106**, 287–300 (2007).
4. Cleveland, W. S. & Loader, C. in *Statistical Theory and Computational Aspects of Smoothing* (eds Härdle, P. D. W. & Schimek, P. D. D. M. G.) 10–49 (Physica-Verlag HD, 1996). at [http://link.springer.com/chapter/10.1007/978-3-642-48425-4\\_2](http://link.springer.com/chapter/10.1007/978-3-642-48425-4_2)